

Comparison of vibrational spectroscopy to biochemical and flow cytometry methods for analysis of the basic biochemical composition of mammalian cells

Judith R. Mourant
Jorge Dominguez
Susan Carpenter
Kurt W. Short
Tamara M. Powers
Ryszard Michalczyk
Nagapratima Kunapareddy
Anabel Guerra
James P. Freyer
Los Alamos National Laboratory
Los Alamos, New Mexico 87545

Abstract. We have conducted an extensive comparison of cellular biochemical composition obtained from infrared and Raman spectra of intact cells with measurements using standard extraction and chemical analysis (including NMR), and flow cytometric assay on fixed cells. Measurements were conducted on a rat fibroblast carcinogenesis model consisting of normal and tumorigenic cells assayed as exponentially growing and plateau-phase cultures. Estimates of protein, DNA, RNA, lipids, and glycogen amounts were obtained from a previous publication in which vibrational spectra were fit to a set of basis spectra representing protein, DNA, RNA, lipids, and glycogen. The Raman spectral estimates of absolute cellular composition were quite similar to the independent biochemical and flow cytometric assays. The infrared spectra gave similar results for protein, lipid, and glycogen but underestimated the DNA content while overestimating the RNA level. When ratios of biochemical concentrations in exponential and plateau-phase cultures were examined, the Raman spectroscopic results were the same, within errors, as the independent methods, in all cases. Several changes in relative biochemical composition due to tumorigenic and proliferative status previously reported using vibrational spectroscopy were confirmed by the independent methods. These results demonstrate that vibrational spectroscopy can provide reliable estimates of the biochemical composition of mammalian cells. © 2006 Society of Photo-Optical Instrumentation Engineers. [DOI: 10.1117/1.2400213]

Keywords: Raman spectroscopy; mid-infrared spectroscopy; biochemical analysis; fibroblast cells; proliferation; tumorigenicity.

Paper 05381RR received Dec. 19, 2005; revised manuscript received Aug. 10, 2006; accepted for publication Aug. 11, 2006; published online Nov. 28, 2006.

1 Introduction

The vibrational spectra of different biochemical molecules are frequently quite distinctive. Consequently, Raman and infrared spectra can be used to estimate the composition of biological cells. There have been many reports of biochemical analysis of cells or tissue based on Raman or infrared spectroscopy. For example, we have published biochemical compositions of fibroblast cells determined by Raman and infrared spectroscopy,^{1,2} biochemical compositions of breast tissue have been reported for several breast tissue pathologies,³ necrotic tissue has been found to contain more cholesterol and cholesterol esters than non-necrotic tissue,⁴ reduced glycogen content and increased nucleic acid content has been reported for malignant as compared to benign prostatic carcinoma,⁵ the DNA content of an apoptotic HeLa cell was found to be 4 to 5 times higher than in the nucleus of a healthy HeLa cell,⁶ the

biochemical composition of coronary arteries have been reported,⁷ the RNA/DNA ratio is greater for neoplastic than normal lymphocytes,⁸ chronic lymphocyte leukemia cells have more DNA and less protein than normal cells,⁹ and the RNA/DNA ratio was observed to increase in H-Ras transfected fibroblast cells.¹⁰

Rarely, however, have the biochemical results of Raman and infrared spectroscopy been verified by biochemical analysis. The one notable exception is a comparison of Raman spectroscopy and biochemical assay results for the biochemical composition of arteries.¹¹ The purpose of the present paper is to compare the results of a recent spectroscopic paper¹ with other biochemical analysis methods to determine the accuracy of the spectroscopic methods. Previously obtained Raman and infrared analyses of protein, lipid, RNA, DNA, and glycogen content in cells are compared with flow cytometry and with extraction and quantification of the biochemicals. Absolute values, ratios of different components within a cell, and ratios

Address all correspondence to Judith R. Mourant, MS E535, Los Alamos National Laboratory, Los Alamos, NM 87545; Tel: 505-665-1190; Fax: 505-665-4637; E-mail: jmourant@lanl.gov

of component concentrations between different cell cultures are all examined.

Potentially, spectroscopic measurements can provide information for cancer diagnosis and treatment monitoring, which is the ultimate aim of this work. Consequently, measurements were performed on a pair of tumorigenic and nontumorigenic cells. Assays were performed on cells from cultures in both the exponential and plateau phases of growth because cell proliferation plays a major role in cancer initiation and progression.

2 Materials and Methods

2.1 Cell Culture

Rat1 cells, derived from rat embryo fibroblast cells by an unknown spontaneous event, are nontumorigenic and immortal. Rat1-T1 fibroblast cells, derived from Rat1 cells by transfection of a mutant *ras* oncogene, are tumorigenic.¹² Monolayer cultures were maintained and subcultured up to 20 passages (cumulative population doublings 120) as described in detail elsewhere.¹² Briefly, cells were cultured as monolayers in standard tissue culture flasks using Dulbeccos Modified Eagles Medium (DMEM, HyClone) containing 4.5 g/l D-glucose, 5% (v/v) fetal calf serum (HyClone), 100 IU/ml penicillin, and 100 μ g/ml streptomycin (HyClone), referred to hereafter as complete medium. Cell suspensions were obtained from monolayer cultures by treating cells with 0.25% trypsin in a phosphate-buffer (pH 7.4) containing 1-mM EDTA and 25-mM HEPES for 10 min. Cold medium was then added. Cell suspensions were passed twice through an 18-gauge needle and centrifuged into a pellet, and the supernatant was removed. After addition of saline, cells were then centrifuged and resuspended in saline at the appropriate concentration and volume for the assays described here.

Previous growth curve experiments showed that monolayers of Rat1 cells reached their growth plateau at ~ 1 to 2×10^5 cells/cm² and Rat1-T1 cells reached confluence at 3 to 5×10^5 cells/cm². Based on these data, exponentially growing cell suspensions were obtained from monolayer cultures harvested at a cell density of less than 1/3 of confluent cultures, while plateau-phase suspensions were obtained from monolayer cultures harvested after 2 to 3 days at confluence with no medium change. The proliferative status of each of these suspensions was confirmed by flow cytometric DNA content analysis as described here.

2.2 Counting/Sizing of the Cells

An aliquot of each cell suspension was counted using an electronic particle counter equipped with a pulse-height analyzer (Z2, Beckman Coulter). Briefly, a cell volume distribution was obtained, and gates were set to select for counting only intact cells, excluding acellular debris. Three counts were taken for each sample and averaged to determine the concentration of cells in the suspension. After counting, a cell volume distribution containing $> 10^4$ cells was saved and processed on a computer to obtain the mean volume of the cells in the suspension. Absolute volumes were determined through calibration of the particle counter using five sizes of polystyrene microspheres (Duke Scientific).

2.3 Standard Flow Cytometry for Determining Cell Cycle

DNA content samples were prepared by fixing 1×10^6 cells in 70% ethanol and then refrigerating. Twenty-four hours prior to analysis, the samples were removed from the refrigerator and centrifuged for 10 min at 1500 xg, pelleting the cells. The ethanol was removed, and the cells were resuspended in a 1-ml solution of 50 μ g/ml propidium iodide (Sigma), 100 μ g/ml RNase A (Sigma), and PBS containing Ca²⁺ and Mg²⁺ (HyClone). After being incubated overnight at 4 °C, the cells were analyzed on a fluorescence-activated flow cytometer, FACS Calibur (Becton-Dickinson), using a 15-mW 488-nm, air-cooled argon-ion laser and a 585-nm emission filter. The data were collected using Cell Quest Software (Becton-Dickinson) and then analyzed using Winlist and ModFit LT (Verity Software House) to determine cell cycle distributions. Debris and aggregates were removed either with a gate in Winlist or by using the debris and aggregates option in ModFit LT.

2.4 Extraction and Quantification of DNA, RNA, and Protein

For each experiment, cells were harvested from cultures growing exponentially and from cultures that had reached a plateau in growth. Six tubes of 2×10^6 cells each (three each plateau and exponential) were used for protein extraction, and 12 tubes of 10^6 cells each were used for DNA and RNA isolation (three each plateau and exponential for both RNA and DNA).

DNA purification was performed with the Wizard SV Genomic DNA purification system (Promega) protocol. Pellets were lysed and transferred to a silica membrane, to which the DNA binds in the presence of chaotropic agents. DNA was washed with SV wash solution (provided in the kit) and then eluted with nuclease-free water at 65 °C. After elution, 2 μ l of RNase was added, and the DNA solution was incubated for 10 min at room temperature. In some experiments, the sample was diluted with 50 mM of Tris HCl before spectroscopic analysis.

RNA isolation was performed using the Perfect RNA Mini kit (Eppendorf). Cells were disrupted with a lysis buffer containing the reducing agent β -mercaptoethanol. After spinning, supernatant was mixed with ethanol and a solution containing guanidine isothiocyanate. This mixture was transferred to the RNA binding matrix. RNA was washed using the washes provided with the kit and finally eluted with molecular-biology-grade water at 50 °C. RNA was diluted with 10 mM or 50 mM Tris HCl before spectroscopic analysis.

Absorbance of the isolated RNA or DNA was measured from 200 to 340 nm. The ratios of absorbance at 260 and 280 nm and at 240 nm and 260 nm were used to monitor for protein contamination in the DNA and RNA samples. Only samples with a 260- to 280-nm absorption ratio higher than 1.5 and for which the absorbance at 240 nm was less than the absorbance at 260 nm were used for quantification. For DNA and RNA samples, absorbance at 260 nm was used to calculate concentration. For DNA, the conversion factor was 1 unit of absorbance at 260 nm = 50 μ g/ml DNA (path length = 1 cm). For RNA, the conversion factor was 1 unit of absorbance at 260 nm = 40 μ g/ml RNA (path length = 1 cm).

A colorimetric assay for protein concentration (DC Protein Assay, Bio-Rad), similar to the well-documented Lowry assay was used. Within 15 min, the reaction reaches 90% of its maximum color development with only a 5% to 10% color change 1 to 2 h after the reagents are added. The reaction of protein with Folin reagent (Reagent B) and an alkaline copper tartrate solution (Reagent A) is the basis of the assay. Color development is the result of a reaction between protein and copper in an alkaline medium and the subsequent reduction of Folin reagent by the copper-treated protein. Tyrosine and tryptophan are primarily responsible for color development, with cystine, cysteine, and histidine also contributing. When the Folin reagent is reduced, it loses 1 to 3 oxygen atoms and turns a characteristic blue color having a maximum absorbance at 750 nm and minimum absorbance at 450 nm.

Tubes of 2×10^6 cells were centrifuged at 14,000 rpm for 2 min, supernatant was removed, 100 μ l of protease inhibitors in radioimmunoprecipitation (RIPA) buffer was added and mixed using a pipette, and the cells left on ice for 25 min with occasional mixing. The cells were then centrifuged at 13,200 rpm at 4 °C for 25 min. 25 or 50 μ l of supernatant of each sample was put into clean tubes prior to adding reagents. At least two sets of 11 BSA (Bovine Serum Albumin, Sigma) standards were used to calibrate the assay: 0, 0.5, 1.0, 1.5, 2.0, 2.5, 3.0, 3.5, 4.0, 4.5, and 5.0 mg/ml. Fresh solutions of BSA in RIPA buffer were made for every experiment.

250 μ l of Reagent A, 2 ml of Reagent B, and 5 μ l of SDS (sodium dodecyl sulfate) were added to each sample, vortexing after each addition. After 15 min, 2 ml of each sample was put into cuvettes, and the absorbances from 745 to 755 nm were read.

For the calculation of the ratio of a biochemical (RNA, DNA, or protein) in exponential and plateau-phase cells, the ratio of the amount of biochemical in exponential and plateau-phase cells was calculated for each experiment, and then these data were averaged and the standard deviation calculated.

2.5 Extraction and Quantification of Glycogen

Cell pellets containing between 0.5 to 1×10^8 cells were assayed for glycogen content using a procedure taken from *Methods for Enzymatic Analysis*, 3rd ed.¹³ The principle steps are

1. Glycogen is hydrolyzed and broken down into glucose molecules by glucoamylase.
2. Glucose is phosphorylated in the presence of adenosine triphosphate (ATP) using hexokinase.
3. NADP^+ is reduced to NADPH by glucose-6-phosphate dehydrogenase, which simultaneously converts glucose-6-P to a lactone.

The amount of glucose liberated by the hydrolysis of glycogen is proportional to the increase of NADPH, measured by the absorbance change at 339 nm. To assure that no signal is obtained from glucose-6-P that might be present at the start of the assay, step 3 is performed before step 2, and a baseline absorbance is measured at that time.

A standard curve was made by measuring known amounts of glycogen in solution using the same absorption measurement protocol as for the cell homogenates. At least two standard solutions were measured each time cell homogenates were run and their absorbance values added to the standard

curve. A straight-line fit of the standard curve yielded concentration as a function of optical absorbance. Glycogen concentrations in the cell pellets were then determined using these results.

For the calculation of the ratio of glycogen in exponential- and plateau-phase cells, the averages and standard deviations of the exponential- and plateau-phase data were individually calculated and then the ratio was computed. The ratio of the averages was then determined and the errors propagated.

2.6 Extraction and Quantification of Lipids

Lipid extraction was performed according to the method of Bligh and Dyer.¹⁴ Cell pellets in the exponential or plateau phase were resuspended in 1 ml PBS (4.85×10^6 to 1.81×10^7 cells), and then 3.75 ml of a mixture of chloroform-methanol (1:2, v:v) was added and vortexed for 10 min. After vortexing, 1.25 ml of chloroform was added and vortexed for 1 min, and then 1.25 ml water was added and vortexed again for 1 min. The system was centrifuged at 3000 rpm for 5 min, and the lower (organic) phase was collected with a syringe and transferred to a small flask. 1.88 ml of chloroform was added to the remaining solution, which was then vortexed for 10 min and centrifuged at 3000 rpm for 5 min. The lower phase was collected and mixed with the first organic phase. The organic phase was evaporated in a rotary evaporator (BÜCHI) and the lipids resuspended in 2 ml of chloroform and stored at -20°C until quantification.

The extracted lipids were quantified using a colorimetric assay.¹⁵ 2 ml of an aqueous solution of ammonium ferri-thiocyanate (FeCl_3 0.1 M, NH_4SCN 0.4 M) was added to glass test tubes, and then 2 ml of lipids in chloroform was added and vigorously vortexed for 1 min. The system was centrifuged at 3000 rpm for 5 min. The lower phase was collected with a syringe, and its absorbance was measured from 200 to 900 nm using pure chloroform as a blank. Absorbance at 465 nm was used for calculations. Solutions of bovine liver lipid extract were used to generate standard curves.

For the calculation of the ratio of lipid in exponential- and plateau-phase cells, the ratio of the amount of biochemical in exponential- and plateau-phase cells was calculated for each experiment, and then these data were averaged and the standard deviation calculated.

2.7 Flow Cytometry for Simultaneous Measurement of Relative Protein, RNA, and DNA Content

To measure protein, the cells were stained with fast green.¹⁶ To measure DNA and RNA, the cells were stained with acridine orange (Calbiochem) using a modification of a published procedure.¹⁷

Tubes containing 10^6 cells previously fixed in 70% ethanol were used in the analysis. Tubes containing the fixed cells were centrifuged at 1500 $\times g$, 4 °C, for 10 min and the ethanol fix discarded. The cell pellets were resuspended in 0.5 ml of distilled water, vortexed gently, and placed on ice. To stain the cells for DNA and RNA, 0.2 ml of a solution of 0.08 M HCl and 0.15 M NaCl in distilled water was added to a tube containing the resuspended cells. After 15 s, 1.2 ml of a solution of 1 mM sodium EDTA, 0.15 M NaCl, 0.037 M citric acid, 0.126 M Na_2HPO_4 , and 12 $\mu\text{g}/\text{ml}$ acridine orange in distilled water was added to the same tube. The tube remained on

ice during these two additions and was not inverted or vortexed. After 5 to 15 min, the same cells were stained for protein using fast green (Polysciences, Inc.). 5 μl from a stock solution of 1 mg/ml fast green in distilled water was added to each tube. The tubes were gently inverted twice to mix the solutions and then placed back on ice for about 1 to 2 h until the flow cytometry analysis.

Flow cytometry was done using a FACS Calibur two-laser flow cytometer (Beckton Dickinson). Acridine orange was excited at 488 nm. The DNA fluorescence was detected at 564 to 606 nm, and the RNA phosphorescence was detected at 653 to 669 nm. Fast green was excited at 633 nm. The protein fluorescence was detected at >670 nm.

The data were analyzed using the program Winlist (Verity Software House). A gate was chosen in Winlist to remove debris and aggregates on a plot of DNA fluorescence area versus DNA fluorescence height. Subsequently, the mean values of the fluorescence signals were computed for DNA, RNA, and protein. To calculate the ratio of biochemical composition in exponential-versus plateau-phase cell cultures, the averages and standard deviations were calculated for each type of cell culture, and then ratios were calculated and the errors propagated through.

2.8 Flow Cytometry for Simultaneous Measurement of Relative Lipid and Protein Content

Cells were stained with Bodipy 493/503 and fast green for measurement of lipid and protein, respectively. Previously fixed samples of 10^6 cells were centrifuged for 10 min at 1500 $\times g$ and 4 °C. The fix solution was discarded, and 1.9 ml of 10 $\mu\text{g}/\text{ml}$ Bodipy 493/503 in PBS was added to each tube. The working Bodipy stain was made from a stock solution of 1 mg/ml in ethanol. The tubes were gently vortexed several times to disperse the cells and incubated at room temperature for 30 to 40 min. The samples were then centrifuged for 10 min at 2000 rpm and at 4 °C, the staining solution poured off, washed with 1.9 ml of cold PBS with gentle vortexing, and centrifuged again at 2000 rpm and at 4 °C. The wash solution was poured off, 1.9 ml of cold PBS added to each tube, and the cells were dispersed by gentle vortexing. 50 μl of 0.1 mg/ml fast green dye in water was then added to each tube. The tubes were inverted twice to mix the contents, covered with foil, and stored in the dark at 4 °C 22 to 26 h before the flow measurements were made. The waiting time of 22 to 26 h was chosen in order to improve the consistency of the lipid results. Data were analyzed using Winlist as described earlier for DNA, RNA, and protein content.

2.9 NMR Spectroscopy

Lipid was extracted, as described earlier, from samples of 1.0×10^8 to 2.5×10^8 cells, and the lipid was stored in 500 μl of chloroform. Before NMR analysis, the chloroform was evaporated and the lipids redissolved in 500 μl of deuteriochloroform (CDCl_3) containing 2.38-mM concentration of triphenylphosphine sulfide ($\text{Ph}_3\text{P}=\text{S}$) as a standard. All NMR spectra were recorded on a Bruker AVANCE 500-MHz spectrometer using a tunable broadband probe. The spectra were processed and analyzed using Bruker XWINNMR 2.6 software.

^1H NMR spectra were recorded with a carrier frequency set at 4.9 ppm and spectral width of 11 ppm using a standard one-pulse sequence. Sixteen scans with 16,000 complex points per spectrum were acquired, and the recycle delay was set to 11.5 s ($>5T_1$) to allow for full relaxation of proton signals. The ^1H T_1 was estimated to be ~ 2 s using an inversion recovery experiment. The spectra were Fourier transformed with 0.5-Hz exponential line broadening and baseline corrected using a second-order polynomial.

^{31}P NMR spectra were recorded with a carrier frequency set at 20 ppm and spectral width of 100 ppm using a standard one-pulse sequence with composite pulse decoupling of protons during acquisition using a WALTZ16 sequence. 1024 or 2048 scans with 32,000 complex points per spectrum were acquired, and the recycle delay was set to 15.8 s ($>5T_1$) to allow for full relaxation of phosphorus signals. The ^{31}P T_1 was estimated to be ~ 2.5 s using an inversion recovery experiment. The spectra were apodized with a 2-Hz exponential function, Fourier transformed, and baseline corrected using a second-order polynomial.

The molar concentration of lipids in the samples was determined using manual integration of proton and phosphorus signals and comparison to the signal integrals of the triphenylphosphine sulfide standard. The concentration of cholesterol was obtained from integration of the methyl proton signal at 0.67 ppm. The concentrations of phospholipids were obtained from integration of phosphorus spectra. The resonance of phosphatidylcholine (PC) was well resolved and was integrated individually; the resonances of phosphatidylethanolamine (PE) and phosphatidylinositol (PI) were broad and overlapping and were integrated together to yield the sum of these two phospholipids (PE+PI). Each spectrum was integrated independently three times to minimize the errors in selection of baseline points. The accuracy of using NMR integrals to determine lipid concentrations was estimated using PC, PE, and PI standards of known concentration. The integration yielded values differing by less than 10% from the actual concentration. The molar concentration was used to calculate the total amount of lipids in each sample using molecular weights of the components of the mixture.

For the calculation of the ratio of lipid in exponential- and plateau-phase cells, the ratio of the amount of biochemical in exponential- and plateau-phase cells was calculated for each experiment, and then these data were averaged and the standard deviation calculated.

2.10 Raman and Infrared Spectroscopy

The details of the Raman and infrared spectroscopy and the analysis methods have been described previously.¹ Only the most important features are stated here. Both the Raman and the Fourier Transform infrared (FTIR) data were taken for cells in phosphate buffered saline (PBS). To facilitate making mid-infrared measurements of aqueous solutions, the data range for the FTIR measurements (1011 to 1575 and 2800 to 2950 cm^{-1}) excluded regions of high water absorption and a path length of 50 μm was used. The dispersive Raman instrument used 785-nm excitation. The regions used for analysis were 450 to 1775 cm^{-1} and 2600 to 3125 cm^{-1} . Both the FTIR and the Raman data were analyzed by fitting the data to a combination of basis spectra including the primary bio-

Table 1 Number of cell preparations used for extraction and quantification.

Cell Type	Protein, RNA, DNA	Lipid (colorimetric)	Glycogen	Lipid (NMR)
Rat1-T1 exponential	4 (5 protein)	7	2	3
Rat1-T1 plateau	4 (5 protein)	7	9	3
Rat1 exponential	6	4	2	0
Rat1 plateau	6	4	4	0

chemical components of cells, DNA, RNA, protein, glycogen, and lipid as described in detail previously.¹

2.11 Summary of Cell Preparations for Biochemical Analysis

Tables 1 and 2 summarize the cell preparations used for biochemical analysis. In most cases, three or more cell preparations were done for each analysis. One exception is the glycogen quantification assay of cells in the exponential phase of growth. The cells used in this paper, as well as the very similar M1 and MR1 fibroblast cells, contain very little glycogen when the cultures are growing exponentially. Since the results for the extractions that were done were both approximately zero, more measurements were not done. The other exception is that NMR quantification of lipids and simultaneous flow cytometry of lipid and protein were performed only for Rat1-T1 cells. The goal of these experiments was to compare various lipid quantification methods that have different sensitivities to different types of lipids. The flow cytometry method is sensitive only to neutral lipids. The NMR method quantitates cholesterol, PE, and the sum of PI plus PC. The colorimetric method has been shown to have different sensitivities to the different phospholipids and is not sensitive to cholesterol.¹⁵

3 Results

3.1 Comparison of Absolute Concentrations

Previously, Raman and infrared spectroscopy were used to estimate the absolute concentrations of protein, lipid, nucleic acids, and glycogen in Rat1 and Rat1-T1 fibroblast cells in both the plateau and exponential phases of growth.¹ In that work, the Raman data from cells were fit to spectra of the basis components. In order to compare those results to the biochemical analysis, the effects of light scattering on the Raman signal intensity must be taken into account. The cells scatter light, which changes the collection efficiency of the Raman system. For example, Raman scattering from a clear solution of protein is stronger than for the same amount of protein in a scattering solution. Several experiments were performed to determine the effect of light scattering by the cells on the collected Raman signal. The spectra were then cor-

Table 2 Number of cell preparations used for spectroscopy and flow cytometry. Flow1 refers to simultaneous flow cytometry of protein, DNA, and RNA content. Flow2 refers to simultaneous flow cytometry on lipid and protein.

Cell Type	Raman	Infrared	Flow1	Flow2
Rat1-T1 exponential	6	11	17	5
Rat1-T1 plateau	4	4	12	5
Rat1 exponential	4	3	5	0
Rat1 plateau	6	11	19	0

rected appropriately. The details of the experiment and the resulting correction factor are given in the appendix.

Figure 1 compares the spectroscopy results with results from extracting and quantifying the biochemical components. The protein concentrations measured by FTIR and Raman spectroscopy are in reasonable agreement with the extracted values, although the FTIR results appear slightly higher. The FTIR and Raman results for lipid match the extracted results fairly well except for one data point. This data point is the

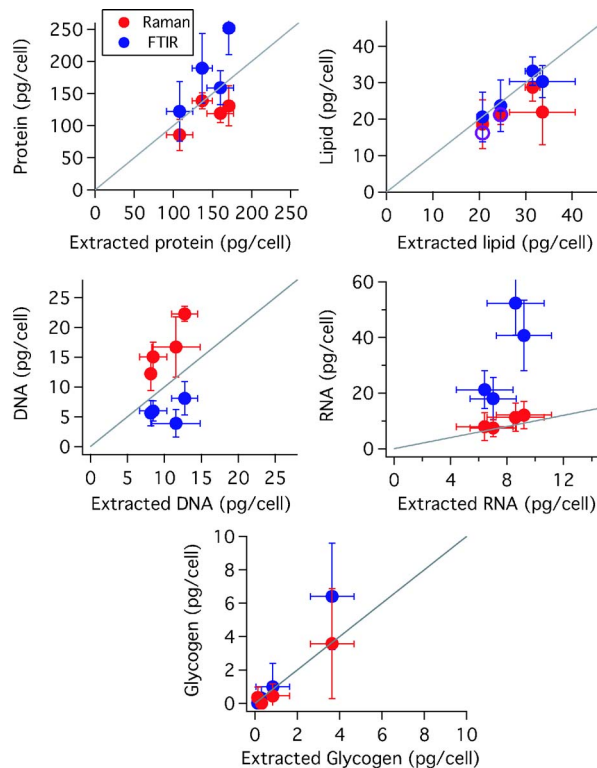


Fig. 1 (Color online) Comparison of spectroscopic measurements of biochemical components with results from extracting and quantifying the biochemicals. The FTIR results are in blue. The Raman results are in red. The gray lines denote the position of perfect correlation. The graph of lipid content also shows NMR results versus extracted results in purple open circles.

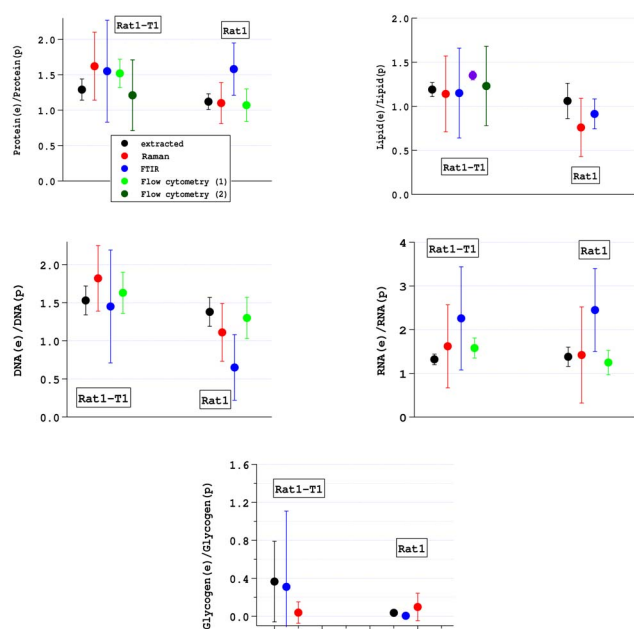


Fig. 2 (Color online) Comparison of the ratio of biochemical components in cells growing in different conditions. The FTIR results are in blue. The Raman results are in red. Extracted and quantitated results are in black. Flow cytometry results obtained when simultaneously measuring protein, DNA, and RNA are in light green. Flow cytometry results obtained when simultaneously measuring protein and lipid are in dark green. NMR results are in purple.

data of Rat1 cells in the plateau phase of growth for which the extracted results have large error bars. The NMR results for Rat1-T1 cells also match the FTIR, Raman, and extracted results. The FTIR results clearly underestimate DNA content and appear to overestimate the RNA content. The Raman results appear to overestimate both DNA and RNA content. We cannot be certain about spectroscopic methods overestimating a biochemical component, because the extracted results may underestimate the concentration of a given biochemical if all of it was not extracted or if there was some loss during the steps before quantitation. For glycogen, there is again a good linear correlation between spectroscopic and extraction results. The FTIR results appear to overestimate the amount of glycogen slightly, while the Raman results agree very well with the extraction results.

3.2 Ratios of Results from Cells Grown under Different Growth Conditions

An advantage of examining the ratio of quantities of biochemicals is that ratios do not depend on the sensitivity of the measurement, but only on the consistency of the measurement. For example, if the extraction and quantification method measures only 90% of the DNA present and the Raman spectroscopy method measures 100% of the DNA, the results for the ratio of DNA in two different samples will still agree.

Cells grown under different conditions can have different biochemical compositions. For example, there is more DNA, on average, in cells in exponentially growing cell cultures than in cells in cultures that have reached a plateau in growth.

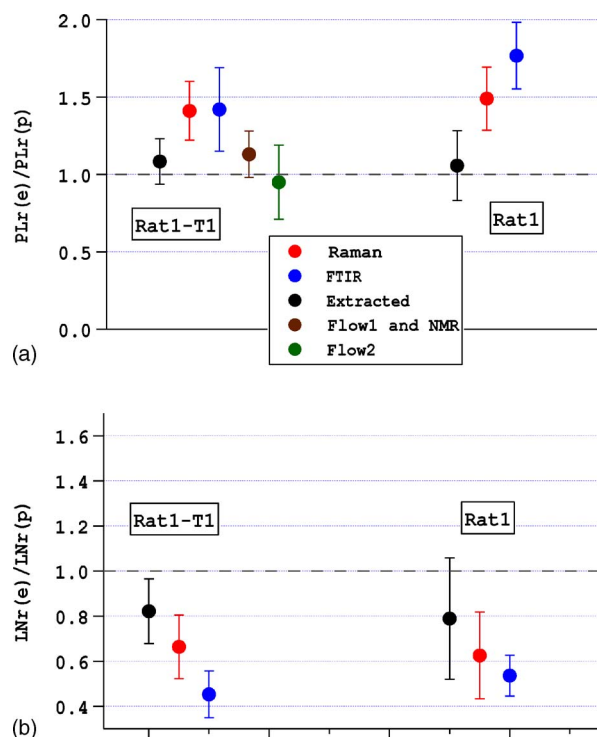


Fig. 3 (Color online) (a) PLr(e) is the ratio of protein to lipid in the exponential phase cell cultures. PLr(p) is the ratio of protein to lipid in the plateau phase cell cultures. (b) LNr(e) is the ratio of lipid to nucleic acids in the exponential phase cell cultures. LNr(p) is the same ratio for the plateau phase cell cultures.

Figure 2 shows ratios of biochemicals in cells from exponential and plateau phases of growth. Results are compared for Raman spectroscopy, infrared spectroscopy, extraction and biochemical or NMR quantitation, and flow cytometry. Averages and standard deviations are shown for all data. In some cases, the average ratio was calculated as the average of the exponential-phase results divided by the average of the plateau-phase results (e.g., the Raman and FTIR results). In other cases, the average ratio is determined from multiple direct measurements of the ratio of biochemical components of exponential- and plateau-phase cells (e.g., extraction and quantification results for protein, lipid, DNA, and RNA, and NMR results for lipid).

The specific question addressed with the data in Fig. 2 is, do spectroscopy results agree with other methods? The answer is yes in nearly all cases. For protein, lipid, RNA, and glycogen, the spectroscopy results have overlapping error bars with the other biochemical methods. For DNA, the error bars overlap for Rat-T1 cells, but the FTIR results and the extraction results have non-overlapping error bars for Rat1 cells.

3.3 Ratios of Biochemical Components within a Cell

A common result presented in spectroscopic analyses is the ratio of biochemicals within a sample, because it is easier to measure relative concentrations than absolute concentrations of biochemicals. Changes in the ratios provide biochemical information that may be used for diagnostic or other medical

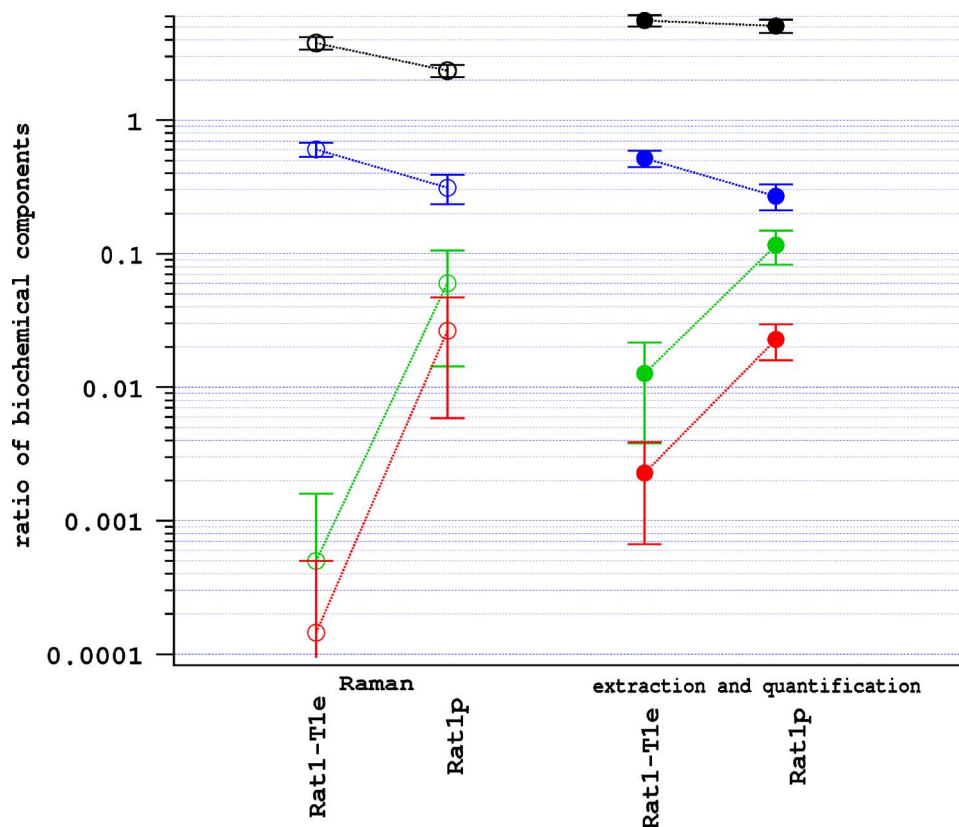


Fig. 4 (Color online) Ratios of biochemical components as determined by Raman spectroscopy (open circles) or extraction followed by quantification (solid circles). The point on the left in each pair is the ratio value for Rat1-T1 cell cultures in the exponential phase of growth; the right point is for Rat1 cell cultures that have reached a growth plateau. Black—protein/lipid; blue—DNA/lipid; green—glycogen/lipid; red—glycogen/protein.

purposes. Consequently, we concentrate on ratios that were found to change outside of the standard deviation by spectroscopic methods.

The spectroscopic results showed that the average protein to lipid ratio, PLr, is greater for the exponential cells. In Fig. 3 (top), the ratio of protein to lipid in exponential-phase cell cultures PLr(e) is divided by the ratio of protein to lipid in plateau-phase cell cultures PLr(p). PLr(e)/PLr(p) is greater than one for all data except for the flow cytometry data on Rat1-T1 cells. However, only the spectroscopic data have error bars that do not overlap with one.

Another spectroscopic result was that the ratio of lipids to nucleic acids, LNr, was different for exponential- and plateau-phase cells. Figure 3 (bottom) demonstrates that LNr(e)/LNr(p) is less than one. The extracted and Raman results agree to within errors; however, the FTIR results are significantly different for Rat1-T1 cells.

In the previous report of spectroscopic results,¹ cancerous tissue was modeled as tumorigenic Rat1-T1 cells in the exponential phase (Rat1-T1e) of growth, and noncancerous tissue was modeled as nontumorigenic Rat1 cells that had reached a plateau in growth (Rat1p). All possible ratios of the five biochemical components measured by Raman spectroscopy were computed for Rat1-T1e cells and Rat1p cells. Four of these ratios were found to be significantly different for the Rat1-T1e and Rat1p cells. These ratios are plotted along with the corresponding results for extraction and quantification in Fig. 4. The Raman measurements for the ratio of protein/lipid are

significantly different for Rat1-T1e and Rat1p. The extraction results show the same trend, but the error bars overlap. For all other ratios, DNA/lipid, glycogen/lipid, and glycogen/protein, the extraction and quantification results verify the changes measured by Raman spectroscopy.

3.4 Verification of Proliferative Status

To verify that the cells were in the expected proliferative state when harvested, cell cycle analyses were performed. The results of cell cycle analyses are the percentages of cells in the G_1 (gap 1), S (synthesis), and G_2 (gap 2) phases of the cell cycle. In the G_1 phase of the cell cycle, there is one copy of the DNA; in the S phase, DNA is being synthesized and there is on average roughly 1.5 times as much DNA as in the G_1 phase; and in the G_2 phase of the cell cycle, there is twice as much DNA as in G_1 . Exponentially growing cell cultures typically have 50% or less of their cells in G_1 , 30 to 40% of their cells in S , and 10 to 15% of the cells in G_2 . Cell cultures that have reached their growth plateau typically have 80% or more of their cells in G_1 , about 10% of their cells in S , and less than 10% of the cells in G_2 . In order to present the data in a succinct form, a metric for DNA content, $G_1\% + 1.5S\% + 2G_2\%$, was calculated. The averages and standard deviations for this metric are given in Tables 3 and 4 for all of the data sets. The cell cycle analyses of cells prepared in the exponential phase of growth are extremely consistent. The cell cycle analyses of the Rat1 cells in plateau are also quite

Table 3 DNA content, $G_1\% + 1.5S\% + 2G_2\%$, for samples used in extractions. Errors shown are standard deviations for three or more measurements.

Cell Type	Protein, RNA, DNA	Lipid (colorimetric)	Glycogen	Lipid (NMR)
Rat1-T1 exponential	131±2	134±4	131	131±1
Rat1-T1 plateau	116±3	117±4	110±3	115±3
Rat1 exponential	133	133±9	131	NA
Rat1 plateau	107±0.3	106±2	107±1	NA

consistent. For the Rat1-T1 cell cultures grown to plateau, the cells used for extraction of protein, RNA, DNA, and lipid were proliferating slightly more than those used for glycogen extraction, Raman and infrared spectroscopy, and flow cytometry of RNA, DNA, and protein.

4 Discussion

4.1 Summary of Primary Results: Comparison of Spectroscopic and Biochemical Results

There is better agreement between Raman and biochemical methods for the measurement of absolute biochemical concentrations than between FTIR and biochemical methods, as evidenced by Sec. 3.1 and Fig. 1. In particular, there appears to be some cross-talk between the RNA and DNA concentrations obtained by FTIR spectroscopy in that DNA concentration is underestimated while RNA concentration is likely overestimated. Finally, the accuracy of the Raman and infrared results is similar to those reported by others (see Table 5 and Sec. 4.5).

For the ratio of a biochemical component concentrations in exponential- and plateau-phase cells, Raman and biochemical assays agree to within errors for all measurements (see Fig. 2). Biochemical and FTIR results are the same to within errors for all but the DNA results for Rat1 cells.

When changes in the ratios of biochemicals between exponential- and plateau-phase cells are considered (Fig. 3), error bars again overlap, with some exceptions for the FTIR and extraction data. For ratios of biochemicals in a tumorigenic and a nontumorigenic model (Fig. 4), the error bars overlap for about 50% of the data. When error bars do not overlap, trends are often the same, such as the greater value of the glycogen to lipid and glycogen to protein ratios for nontumorigenic plateau-phase cells.

The biochemical assays verify several spectroscopic results. The verified Raman spectroscopic results are as follows: For Rat1-T1 cells, there is more protein and more DNA in cells from exponentially growing cultures than in cells from cultures that reached the growth plateau. For both Rat1 and Rat-T1 cells, there is less glycogen in cells from exponentially growing cultures than in cells from cultures that reached the growth plateau. The ratio of lipids to nucleic acids is smaller for exponentially growing Rat1-T1 cell cultures than for cell

Table 4 DNA content, $G_1\% + 1.5S\% + 2G_2\%$, for Raman, infrared, and flow cytometry samples. Flow1 refers to the samples used for simultaneous analysis of RNA, DNA, and protein. Flow2 refers to the samples used for simultaneous analysis of protein and lipid.

Cell Type	Raman	Infrared	Flow1	Flow2
Rat1-T1 exponential	131±2	132±2	132±2	132±2
Rat1-T1 plateau	111±4	111±4	108±4	115±3
Rat1 exponential	132±2	131±1	130±2	NA
Rat1 plateau	110±6	110±3	110±3	NA

cultures in the plateau phase. The DNA to lipid ratio is greater, and the glycogen to lipid and glycogen to protein ratios are less for exponentially growing Rat1-T1 cells than for plateau-phase Rat1 cells.

4.2 Lipid Quantification

As noted in the methods section, several methods of lipid quantification were used. NMR spectroscopy specifically measured cholesterol concentration plus the sum of the concentrations of PC, PI, and PE. The optical spectroscopy and the colorimetric assay were referenced to a commercially obtained liver lipid extract, and the flow cytometry assay measured only neutral lipids. In Fig. 2, it can be seen that the NMR assay yielded a larger value for the ratio of lipid in cells from exponential- and plateau-phase cultures than did the colorimetric assay. One possible cause for this result is that the composition of lipids in exponential- and plateau-phase cell cultures differs. We are currently investigating this possibility. The error bars on the flow cytometry and optical spectroscopy results were large enough that it was not possible to determine if the results of these assays differed significantly from each other or from the other assays.

Table 5 The root-mean-square-error (RMSE) for using Raman or infrared spectroscopy to determine protein, lipid, or glycogen concentrations in cells. Last two columns: the range of concentrations measured in cell suspensions divided by the RMSE.

Cell Type	RMSE (mg/dL)		Range / RMSE	
	Raman	Infrared	Raman	Infrared
Protein	1000	974	3.2	1.3
Lipid	315	38	2.0	6.8
Glycogen	17	28	10.4	2.5

4.3 Sources of Error in Reference Measurements

None of the biochemical methods used in this work are perfect. All methods using extracted biochemicals are sensitive to whether all of the biochemical is extracted. Therefore, when the spectroscopic results give larger values than the extraction methods, it is possible that it is the biochemical method that is in error rather than the spectroscopic method. The protein and lipid assays can have additional errors because they are sensitive to the distribution of types of proteins and lipids present. The effects of this on lipid results were discussed in detail earlier. In the case of protein, spectroscopic measurements of extracted protein did not show any differences in protein composition for the cell cultures used in this work.¹ Therefore, the sensitivity of the protein assay to the types of protein present was probably not a significant source of error. Finally, flow cytometry results can depend on staining conditions. Although all attempts were made to standardize staining procedures, variations can lead to larger standard deviation such as the greater standard deviation seen for some of the flow results in Fig. 2 for protein.

4.4 Effects of Performing Analyses on Cell Cultures Prepared at Different Times

Most work comparing spectroscopy with biochemical/clinical assays compares measurements on individual samples. This was not done, for some practical reasons. Several of the extraction/quantification and flow cytometry assays that were run are not standard techniques and were not developed at the time the Raman and infrared measurements were performed. Second, it was found that all of the extraction assays gave larger yields and were more reproducible when performed on fresh cells. To perform the spectroscopy and all of the extraction/quantification assays on the same day is not feasible.

The cell cycle analyses demonstrate that the preparations of exponential phase cells were quite consistent, as were the preparations of the Rat1 cells in the plateau phase of growth. There was a small variation in the preparation of the Rat1-T1 plateau cells (Sec. 3.4, Table 3), which could have lead to slightly increased concentrations of protein, lipid, DNA, and RNA in the extractions. This error would in turn lead to low values of the ratio of these biochemicals in exponential- and plateau-phase cells. Consistent with this, the data in Fig. 2 show that the average ratio of protein in exponential- and plateau-phase cells was lower for the data taken using cell plateau cultures that had a large value of the DNA metric.

4.5 Other Studies Comparing Raman and Infrared Spectroscopy to Biochemical Assays

Raman spectroscopy has been used to assay the biochemical composition of arteries and the results compared with standard biochemical methods.¹¹ In that work, the Raman spectra of minced artery (and in some cases, adventitia) tissue were fit to a linear combination of basis spectra of beta-carotene, calcium salts, extracted fat, a spectrum of cholesterol in the presence of fatty acids, free cholesterol, and two different spectra of delipidized artery. The accuracy of results for free cholesterol, esterified cholesterol, extracted fat, and calcium salt content was then investigated by comparison to results from extracting these compounds. For example, the percentage of

the tissue that was free cholesterol, as determined by Raman spectroscopy, was plotted against the percent of free cholesterol, as determined by extracting and weighing free cholesterol. For total lipids and the two forms of cholesterol, the correlation coefficient ranged from 0.848 to 0.998. The slopes of lines fit to the data varied from 0.75 to 1.2. For calcium salts, the Raman results were divided by a factor of 1.5 (of unknown origin), and then a correlation coefficient of 0.994 and a slope of 1.5 was obtained. No comparison to biochemical results was performed for beta-carotene or delipidized artery. These results are qualitatively similar to those reported in the present work, but with some important differences. The biological system is quite different. The ability to use basis spectra in the analysis of Raman data of arteries does not mean that a basis-spectra-based analysis of Raman spectra cells will provide accurate results (and vice versa). The basis spectra used by Brennan et al.¹¹ were quite different from the basis spectra used in the present work. Reference 11 focused on lipids, cholesterol, and calcium salts, whereas the present work examines the accuracy of determination of different biochemical components, i.e., protein, RNA, DNA, and glycogen.

Raman and infrared measurements of concentrations of serum, urine, and plasma constituents have been compared to standard clinical measurements of the same components.¹⁸⁻²² In all but one case, the infrared and Raman spectra were analyzed using partial least squares (PLS) to determine component concentrations (e.g., total protein, triglycerides, cholesterol, HDL, LDL, glucose, urea, and uric acid). The PLS method has the advantage that component concentrations can be determined even if all of the significantly contributing biochemical components are not known. However, it has the disadvantage that a training set must be used that represents the total variability that will be found in the samples. It can be very difficult to obtain such a training set and to prove that it represents the variability of the set of all human serum samples. The data analysis method for one of the papers reporting FTIR spectroscopy of plasma samples used component spectra.²¹ Basically, spectral regions dominated by each component were determined. Subsequently, using these spectral regions, the component with the largest contribution to the spectrum was determined and its spectrum subtracted from the plasma spectrum. This procedure was repeated iteratively for all components. Although the methods of analysis of the serum, urine, and plasma samples is somewhat different from the method discussed in this paper, all techniques of determining concentrations via vibrational spectroscopy rely on the distinctiveness of the spectra of the biochemical compounds such as protein and lipid.

Results of the urine, serum, and plasma studies have been presented in terms of root-mean-square-error (RMSE) of prediction, and a summary of the serum studies using FTIR and Raman spectroscopy is provided by Rohleder et al.¹⁹ The lowest errors were obtained for uric acid, with an RMSE of 1.1 to 2.4 mg/dL for the Raman studies cited. The largest errors are for protein. For the two FTIR studies, RMSEs of 71 mg/dL and 176 mg/dL were obtained. For Raman spectroscopy, the RMSEs ranged from 280 to 328 mg/dL. For the FTIR study of urine, an RMSE of 48 mg/dL was obtained. For the

plasma study, an RMSE for albumin (the primary protein constituent) of 166 mg/dL was obtained.

The calibration step in PLS nearly eliminates differences in the spectroscopic and clinical/biochemical methods due to systematic errors in the clinical/biochemical methods such as not extracting all of the material of interest. Consequently, the reported RMSEs are expected to be lower than for the data presented in this paper. Table 5 provides RMSEs for the data in Fig. 1 assuming that the assay method was perfect. The cell concentration for the Raman measurements was estimated to be $\sim 5 \times 10^8$ cells/ml, while the cell concentration for the infrared measurements was estimated to be $\sim 2 \times 10^8$ cells/ml. Data are not presented for RNA and DNA, as there was a large discrepancy between absolute values for the extraction, FTIR, and Raman methods.

More important than the absolute error is the ratio of the range of concentrations of an analyte compared to the RMSE of prediction. This number has been found to vary from 1.5 for glucose to 9.5 for total protein in a Raman spectroscopy study of serum.¹⁸ For the FTIR study of plasma, values of 18.0 and 21.8 were obtained for albumin and glucose.²¹ For the FTIR study of urine,²² the range of concentrations divided by the RMSE was ~ 13.5 . Results from the present work are presented in Table 5 and are similar to those of the other studies.

5 Conclusions

In order for vibrational spectroscopy to meet its full potential of noninvasively providing biochemical information about biological cells and tissue, the accuracy of the technique must be proven. This paper addresses the specific question of whether the biochemical content of mammalian cells can be determined by fitting the vibrational spectra to a set of basis spectra plus fluorescence and background (e.g., saline). Similar models have been used for analyzing Raman spectra of arteries and the accuracy of the model determined for most but not all of the components.¹¹ In this work, we have examined a very different biological system, cells alone, and determined the accuracy to which the concentration of all of the biochemicals in the model (protein, lipid, RNA, DNA, and glycogen) were determined. Results for both absolute concentration as well as for relative concentrations demonstrate good agreement between the biochemical and spectroscopic methods. When absolute concentrations are used, the error bars are frequently larger for the spectroscopic techniques. However, when ratios of biochemicals within cells are considered, the error bars are similar for the spectroscopic and biochemical results.

The results demonstrate that the effect of light scattering on the Raman signal must be taken into account in some cases, such as when absolute quantification of biochemical content is needed. The intensity of the Raman scattered light depends on the scattering properties of the medium.

This model of using protein, lipid, RNA, DNA, and glycogen spectra should be applicable to a wide variety of cells, although care must be taken to assure that the lipid and protein spectra used are representative of the cells being analyzed. Furthermore, since epithelial tissue is primarily comprised of cells, Raman spectroscopy should be able to noninvasively provide biochemical information about the cel-

lular epithelium where most cancers originate. The range of concentrations measured will potentially be greater in tissue as the biochemical variation of tissue pathologies is expected to be larger than for the model systems used in this work, and consequently range/RMSE values shown in Table 5 will increase.

Two specific questions were addressed in this paper:

- Do spectroscopy results agree with other methods of determining biochemical composition?
- Are the spectroscopy methods accurate enough to detect differences between biological systems?

The answer to both questions is yes. The strength of vibrational spectroscopy lies in measurements where ratios of biochemicals within cells are important. Challenges lie in applying the model to tissue and determining if the biochemical changes measured are relevant to pathology.

6 Appendix

This appendix discusses the effects of light scattering on the intensity of the Raman signal and how this phenomenon affects the determination of biochemical concentrations. The basis spectra for protein, DNA, RNA, and glycogen were obtained by measuring clear solutions of known concentrations of each compound. In contrast to these nonscattering solutions, the cells that contain these components scatter light. The cell suspensions measured for this work appeared turbid and have reduced scattering coefficients of about 4 cm^{-1} (unpublished data obtained using the method of oblique incidence).²³ To use the basis spectra to determine the biochemical composition of the cells, it was necessary to know how the scattering properties of the cells affected the intensity of the scattered light. Consequently, an experiment was performed to determine how the light scattering of cells affects the Raman intensity. A clear solution of glycogen was prepared by adding $50 \mu\text{l}$ of 600 mg/ml glycogen to $750 \mu\text{l}$ of saline. The Raman spectrum was then determined. Rat-T1 cells were prepared for spectroscopy,¹ and the Raman spectrum of $750 \mu\text{l}$ of centrifuged cells was determined. Subsequently, $50 \mu\text{l}$ of 600 mg/ml glycogen was added to the $750 \mu\text{l}$ of cells. The Raman spectrum of this sample was measured. The Raman spectrum of glycogen could then be determined by subtracting the spectrum of only cells. From these measurements, the intensity of the Raman spectrum of pure glycogen (37.5 mg/ml) was found to be a factor of 1.75 greater than the intensity of the Raman spectrum of glycogen added to the cell suspension (also 37.5 mg/ml). The concentration of glycogen occurring naturally in the cells used in this experiment was about 0.5 mg/ml. Since this concentration is much less than the concentration of glycogen that was added to the cells and it was subtracted out by subtracting out the cells-only spectrum, it should not have interfered with the measurements.

The basis spectra for lipid used in this work was obtained by suspending liver lipid extract in an aqueous solution.¹ The suspension was scattering, since micelles of a variety of sizes were present. For this work, the scattering properties of the lipid suspension were assumed to be similar enough to the scattering properties of the cells that no corrections of the concentration of lipid obtained by fitting the cell data were needed. This assumption was based on the fact that the inten-

sity of the Raman spectra does not depend strongly on the exact scattering properties of the medium. When the previously described experiment with cells and glycogen was performed with cells and polystyrene spheres (0.12 μm diam), a correction factor of 2 was obtained rather than 1.75. A monodisperse suspension of polystyrene spheres ($n \sim 1.58$) has somewhat different light-scattering properties than cells that contain a wide variety of scatter sizes that have much smaller indices of refraction ($n \sim 1.38$).²⁴ Additionally, in measurements of glycogen added to a suspension of polystyrene spheres, the Raman intensity of glycogen was found to decrease only weakly with added scattering (i.e., more polystyrene spheres) after a reduced scattering coefficient of 2 cm^{-1} was reached. A scattering increase from 2 to 5 cm^{-1} results in a signal decrease of only 6%, which equates to 3.4% of the original signal.

In conclusion, the effect of scattering on the intensity of Raman scattered light can be significant. The exact effect on the Raman intensity will depend on the measurement geometry and will likely be different for other probe geometries.

Acknowledgments

The authors gratefully acknowledge funding through the NIH NCI (Grant No. CA89255) and use of the NIH National Flow Cytometry Resource (Grant No. RR01315). We would like to thank Leslie Coburn for some of the original work evaluating DNA and RNA extraction kits and Antoinette Trujillo for support on some of the Raman experiments reported in the appendix.

References

1. J. R. Mourant, K. W. Short, S. Carpenter, N. Kunapareddy, L. Coburn, T. M. Powers, and J. P. Freyer, "Biochemical differences in tumorigenic and nontumorigenic cells measured by Raman and infrared spectroscopy," *J. Biomed. Opt.* **10**, 031106 (2005).
2. K. W. Short, S. Carpenter, J. P. Freyer, and J. R. Mourant, "Raman spectroscopy detects biochemical changes due to proliferation in mammalian cell cultures," *Biophys. J.* **88**, 4274–4288 (2005).
3. A. S. Haka, K. E. Shafer-Peltier, M. Fitzmaurice, J. Crowe, R. R. Dasari, and M. S. Feld, "Diagnosing breast cancer by using Raman spectroscopy," *Proc. Natl. Acad. Sci. U.S.A.* **35**, 12371–12376 (2005).
4. S. Koljenivic, L.-P. Choo-Smith, T. C. Bakker Schut, J. M. Kros, H. J. van den Berge, and G. J. Puppels, "Discriminating vital tumor from necrosis tissue in human glioblastoma tissue samples by Raman spectroscopy," *Lab. Invest.* **82**, 1265–1277 (2002).
5. P. Crow, N. Stone, C. A. Kendall, J. S. Uff, J. A. M. Farmer, H. Barr, and M. P. J. Wright, "The use of Raman spectroscopy to identify and grade prostatic adenocarcinoma *in vitro*," *B. J. Cancer Research* **89**, 106–108 (2003).
6. N. Unzabakava, A. Lenferink, Y. Kraan, E. Volokhina, G. Vrensen, J. Greve, and C. Otto, "Nonresonant confocal Raman imaging of DNA and protein distribution in apoptotic cells," *Biophys. J.* **84**, 3968–3981 (2003).
7. T. J. Römer, J. F. Brennan, M. Fitzmaurice, L. Feldstein, G. Deinum, J. L. Myles, J. R. Kramer, R. S. Lees, and M. S. Feld, "Histopathology of human coronary atherosclerosis by quantifying its chemical composition with Raman spectroscopy," *Circulation* **97**, 878–885 (1998).
8. E. Benedetti, E. Bramanti, F. Papineschi, I. Rossi, and E. Benedetti, "Determination of the relative amount of nucleic acids and proteins in leukemic and normal lymphocytes by means of Fourier transform infrared microspectroscopy," *Appl. Spectrosc.* **51**, 792–797 (1997).
9. C. P. Schultz, K. Liu, J. B. Johnston, and H. H. Mantsch, "Study of chronic lymphocytic leukemia cells by FT-IR spectroscopy and cluster analysis," *Leuk. Res.* **20**, 649–655 (1996).
10. J. Ramesh, A. Salman, Z. Hammody, B. Cohen, J. Gopas, N. Grossman, and S. Mordachai, "FTIR microscopic studies on normal and H-Ras oncogene transfected cultured mouse fibroblasts," *Eur. Biophys. J.* **30**, 250–255 (2001).
11. J. F. Brennan, T. J. Römer, R. S. Lees, A. M. Tercyak, J. R. Kramer, and M. S. Feld, "Determination of human coronary artery composition by Raman spectroscopy," *Circulation* **96**, 99–105 (1997).
12. L. A. Kunz-Schughart, A. Simm, and W. Mueller-Klieser, "Oncogene-associated transformation of rodent fibroblasts is accompanied by large morphologic and metabolic alterations," *Oncol. Rep.* **2**, 651–661 (1995).
13. D. Keppler and K. Decker, "Glycogen," in *Methods of Enzymatic Analysis*, 3rd ed., Vol. 6, H. U. Bergmeyer, Ed., pp. 11–18, Verlag Chemie GmbH, Weinheim, Germany (1983).
14. E. G. Blich and W. J. Dyer, "A rapid method for total lipid extraction and purification," *Can. J. Biochem. Physiol.* **37**, 911–917 (1959).
15. J. C. Stewart, "Colorimetric determination of phospholipids with ammonium ferriethoxyanate," *Anal. Biochem.* **104**, 10–14 (1980).
16. C. M. Wilson, "Studies and critique of amido black 10B, coomassie blue R, and fast green FCF as stains for proteins after polyacrylamide gel electrophoresis," *Anal. Biochem.* **96**, 263–278 (1979).
17. Z. Darzynkiewicz, "Differential staining of DNA and RNA in intact cells and isolated cell nuclei with acridine orange," *Methods Cell Biol.* **33**, 285–298 (1990).
18. A. J. Berger, T.-W. Koo, I. Itzkan, G. Horowitz, and M. S. Feld, "Multicomponent blood analysis by near-infrared Raman spectroscopy," *Appl. Opt.* **38**, 2916–2926 (1999).
19. D. Rohleder, G. Kocherscheidt, K. Gerber, W. Keifer, W. Köhler, J. Möcks, and W. Petrich, "Comparison of mid-infrared and Raman spectroscopy in the quantitative analysis of serum," *J. Biomed. Opt.* **10**, 031108-1–031108-9 (2005).
20. J. Y. Qu, B. C. Wilson, and D. Suria, "Concentration measurements of multiple analytes in human sera by near-infrared laser Raman spectroscopy," *Appl. Opt.* **38**, 5491–5498 (1999).
21. C. Petibois, G. Cazorla, A. Cassaigne, and G. Deleris, "Plasma protein contents determined by Fourier-transform infrared spectrometry," *Clin. Chem.* **47**, 730–738 (2001).
22. R. A. Shaw, S. Low-Ying, M. Leroux, and H. H. Mantsch, "Toward reagent-free clinical analysis: quantitation of urine urea, creatine, and total protein from the mid-infrared spectra of dried urine films," *Clin. Chem.* **46**, 1493–1495 (2000).
23. L.-H. Wang and S. L. Jacques, "Use of a laser beam with an oblique angle of incidence to measure the reduced scattering coefficient of a turbid medium," *Appl. Opt.* **34**, 2362–2366 (1995).
24. J. R. Mourant, T. M. Johnson, S. Carpenter, A. Guerra, and J. P. Freyer, "Polarized angular dependent spectroscopy of epithelial cells and epithelial nuclei to determine the size scale of scattering structures," *J. Biomed. Opt.* **7**, 378–387 (2002).